Estimation of dairy goat body composition: A direct calibration and comparison of eight methods

Sylvain Lerch, Anne de La Torre, Christophe Huau, Mathieu Monziols, Caroline Xavier, Loïc Louis, Yannick Le Cozler, Philippe Faverdin, Philippe Lamberton, Isabelle Chery, et al.

Methods xxx (xxxx) xxx–xxx

Contents lists available at ScienceDirect

Methods

journal homepage: www.elsevier.com/locate/ymeth

Estimation of dairy goat body composition: A direct calibration and comparison of eight methods☆

Sylvain Lerch[a,*], Anne De La Torre[b], Christophe Huau[c], Mathieu Monziols[d], Caroline Xavier[a,e], Loïc Louis[f], Yannick Le Cozler[e], Philippe Faverdin[e], Philippe Lamberton[e], Isabelle Chery[g], Dominique Heimo[h], Christelle Loncke[i], Philippe Schmidely[i], José A.A. Pires[b,*]

[a] Agroscope, Ruminant Research Unit, Route de la Tioleyre 4, 1725 Posieux, Switzerland
[b] INRAE, Université Clermont Auvergne, Vetagro Sup, UMR Herbivores, 63122 Saint-Genès-Champanelle, France
[c] GenPhySE, Université de Toulouse, INRAE, ENVT, 31326 Castanet-Tolosan, France
[d] IFIP institut du porc, 35650 Le Rheu, France
[e] PEGASE, INRAE, Institut Agro, 35590 Saint Gilles, France
[f] Université de Lorraine, AgroParisTech, INRAE, SILVA, 54000 Nancy, France
[g] IPHC, CNRS, Université de Strasbourg, 67037 Strasbourg, France
[h] Agroscope, Feed Chemistry Unit, Route de la Tioleyre 4, 1725 Posieux, Switzerland
[i] Université Paris-Saclay, INRAE, AgroParisTech, UMR Modélisation Systémique Appliquée aux Ruminants, 75005 Paris, France

ARTICLE INFO

Keywords:
Ruminant
Body chemical composition
3D imaging
Computer tomography
Adipose cell size
Deuterium oxide

ABSTRACT

The objective was to compare eight methods for estimation of dairy goat body composition, by calibrating against chemical composition (water, lipid, protein, mineral and energy) measured *post-mortem*. The methods tested on 20 Alpine goats were body condition score (BCS), 3-dimension imaging (3D) automatic assessment of BCS or whole body scan, ultrasound, computer tomography (CT), adipose cell diameter, deuterium oxide dilution space (D_2OS) and bioelectrical impedance spectroscopy (BIS). Regressions were tested between predictive variates derived from the methods and empty body (EB) composition. The best equations for estimation of EB lipid mass included BW combined with i) perirenal adipose tissue mass and cell diameter (R^2 = 0.95, residual standard deviation, rSD = 0.57 kg), ii) volume of fatty tissues measured by CT (R^2 = 0.92, rSD = 0.76 kg), iii) D_2OS (R^2 = 0.91, rSD = 0.85 kg), and iv) resistance at infinite frequency from BIS (R^2 = 0.87, rSD = 1.09 kg). The D_2OS combined with BW provided the best equation for EB protein mass (R^2 = 0.97, rSD = 0.17 kg), whereas BW alone provided a fair estimate (R^2 = 0.92, rSD = 0.25 kg). Sternal BCS combined with BW provided good estimation of EB lipid and protein mass (R^2 = 0.80 and 0.95, rSD = 1.27 and 0.22 kg, respectively). Compared to manual BCS, BCS by 3D slightly decreased the precision of the predictive equation for EB lipid (R^2 = 0.74, rSD = 1.46 kg), and did not improve the estimation of EB protein compared with BW alone. Ultrasound measurements and whole body 3D imaging methods were not satisfactory estimators of body composition ($R^2 \leq 0.40$). Further developments in body composition techniques may contribute for high-throughput phenotyping of robustness.

Abbreviations: ACD, adipose cell diameter; 3D, three-dimension; BCS, body condition score; BIS, bioelectrical impedance spectroscopy; BW, body weight; CT, computer-tomography; CV, coefficient of variation; D_2O, deuterium oxide; D_2OS, deuterium oxide dilution space; DM, dry matter; EB, empty body; IRMS, isotope ratio mass spectrometry; R, resistance; rCV, residual coefficient of variation; rSD, residual standard deviation; SD, standard deviation; US, ultrasound; Xc, reactance

☆ Dedicated to the memory of François Bocquier

* Corresponding authors.
E-mail addresses: sylvain.lerch@agroscope.admin.ch (S. Lerch), anne.de-la-torre-capitan@inrae.fr (A. De La Torre), christophe.huau@inrae.fr (C. Huau), mathieu.monziols@ifip.asso.fr (M. Monziols), caroline.xavier@agroscope.admin.ch, caroline.xavier@agrocampus-ouest.fr (C. Xavier), loic.louis@inrae.fr (L. Louis), yannick.lecozler@agrocampus-ouest.fr (Y. Le Cozler), philippe.faverdin@inrae.fr (P. Faverdin), philippe.lamberton@inrae.fr (P. Lamberton), isabelle.chery@iphc.cnrs.fr (I. Chery), dominique.heimo@agroscope.admin.ch (D. Heimo), christelle.loncke@agroparistech.fr (C. Loncke), philippe.schmidely@agroparistech.fr (P. Schmidely), jose.pires@inrae.fr (J.A.A. Pires).

https://doi.org/10.1016/j.ymeth.2020.06.014
Received 13 May 2020; Received in revised form 21 June 2020; Accepted 22 June 2020

1. Introduction

The management of body reserve accretion and mobilization throughout growth and gestation - lactation cycles is a major determinant of ruminant adaptation capacity to changing environments and thus lifetime productivity [1]. Furthermore, the dynamics of accretion and mobilization of body lipids regulate biological functions (e.g., growth, lactation, reproduction) by influencing the animal physiology and metabolic health, driving the flow of lipophilic molecules (fatty acids, vitamins, contaminants, drugs) to animal products, thus modulating their nutritional quality and safety. Therefore, precise phenotyping of body composition (lipid, protein, minerals and energy) and its variation over time are indispensable in animal research, for instance, to assess adaptation of different genotypes to changing environments and production systems.

Direct measurements of body composition *via* slaughter, dissection and chemical analyses remain the "gold standard" (i.e. the reference methodology) but are not compatible with longitudinal studies. Over the past century, several methods were developed or adapted to estimate livestock body composition *in vivo*, that vary in invasiveness, acquisition time, cost, sensitivity and feasibility. They are mainly based on four basic principles:

i) Assessment of external shape and/or subcutaneous tissues [body condition score (BCS), 3D imaging and ultrasound (US)] [2,3],
ii) Measurement of tissue and organ volume or mass by quantification of the attenuation of radiation or electromagnetic field (computer tomography (CT) and dual-energy X-ray absorptiometry, magnetic resonance imaging) [4],
iii) Measurement of the adipose cell diameter (ACD), that is linked with total empty body (EB) lipid mass [5,6],
iv) Direct quantification of water mass, by dilution space of deuterium oxide (D_2OS) or other markers [7,8], or indirect assessment of body water by determining body resistance to electrical current (BIS, [9])) or sound (velocity of sound, [10]).

Relatively few experiments compared the gold standard of chemical composition measured *post-mortem* with a large set of methods for *in vivo* estimation of body composition. Those comparisons are mostly limited to three or less methods (e.g. in goats: ACD, BCS and US [11], and D_2OS, urea dilution space and BCS [12]; in ewes: D_2OS, ACD and BCS [6]). Direct calibration and comparison are required to evaluate the relative precision of the different methods tested, and their respective advantages and limits to estimate *in vivo* body composition in animal research.

The objective was to compare eight methods for estimation of dairy goat composition: deuterium oxide dilution space (D_2OS), bioelectrical impedance spectroscopy (BIS), adipose cell diameter (ACD), body condition score (BCS), 3-dimension (3D) whole body scan or automatic assessment of BCS (3D-BCS), ultrasound (US) and computer tomography (CT), by calibrating them against chemical composition measured *post-mortem*.

2. Materials and methods

2.1. Animals

All procedures performed on animals were approved by the Ethics Committee on Animal Experimentation and the French Ministry of Higher Education, Research and Innovation (APAFiS#15681-2018062622272488_v2). The experiment was conducted at the INRAE experimental farm "Installation Expérimentale en Production du Lait" (PEGASE, INRAE, Institut Agro, 35590 Saint-Gilles, France).

Twenty Alpine goats (3.0 ± 0.6 years old; 226 ± 9 days in milk) weighing 47 to 72 kg were used in this experiment. Goats were milked once a day at approximately 0800 h. Hay was distributed at 0900 h and 1600 h and concentrate (750 g/d) was offered individually in the milking parlor. Goats were housed in a free stall barn on barley straw bedding and had free access to hay and water. Goat characteristics, milk yield and composition are reported in Table 1.

Table 1
Goats (n = 20) characteristics and milk production and composition.

Item	Mean	SD	Min	Max
Age, years	3.0	0.6	2.6	4.6
Parity	2.3	0.6	2	4
Days in milk	226	9.3	211	239
Reference BW, kg[1]	56.5	7.7	46.7	72.0
Milk yield, kg.d^{-1}	1.07	0.32	0.07	1.54
Milk composition[2]				
Fat, %	4.42	6.67	33.53	58.2
Protein, %	4.23	3.59	33.63	47.77
Lactose, %	3.98	2.79	34.88	45.05
SCC[3] (×1000)	4949	1982	629	8247

[1] Reference body weight (BW): average of measurements on days - 2 and - 1 of the experiment used to calculate the amount of D_2O to administer.
[2] Milk composition was determined by mid-infrared spectroscopy (Lillab, Châteaugiron, France).
[3] SCC: Somatic cells count.

2.2. Methods for body composition estimation

The experiment was conducted in two successive calendar weeks, from −3 to +9 days relative to the D_2O injection (day 0). The timeline of measurements is reported in Fig. 1.

2.2.1. Body weight, BCS and body measurements

Body weight (BW) was recorded in the morning, after milking and before hay distribution, five times during the study (Fig. 1). The BCS was assessed by a trained scorer on day 4 of the experiment, using a 0 to 5 scale with quarter-point intervals, and based on visual evaluation and palpation of sternal and lumbar regions [13]. Seven morphological traits were measured on live goats on day 3 of the experiment: 1. Height-at–withers (distance from the floor to the withers); 2. Length vertex-tail (distance from the external occipital protuberance to the base of the tail); 3. Body length (distance between the point of the shoulder to the right tuber ischia); 4. Chest depth (maximal distance of the thoracic cage); chest girth, measured at 3 locations (5. Heart girth behind the front legs and withers; 6. Middle girth after the 13th rib and 7. Rear girth before the hips and mammary gland). A height gauge was used to measure height-at-withers and chest depth. A metric tape was used for the other measurements (see Supplementary file S1 for precise illustrations of measurement locations).

2.2.2. Deuterium oxide dilution space (D_2OS)

Goats were fitted with a temporary jugular catheter (Intraflon 2, PTFE, 16 G × 60 mm, Ecouen, France) and injected with a D_2O bolus (0.2 ± 0.008 g D_2O.kg BW^{-1}; 99.97%, Euriso-top, Saint-Aubin, France) at 1114 h (± 13 min) of day 0 (Fig. 1). The catheter was then flushed with 10 mL of saline solution (0.9% NaCl; Lavoisier, Paris, France) and immediately removed.

The mass of D_2O to administer was determined precisely by weighing syringes (BD Medical, Le Pont-de-Claix, France) before and after injection to the nearest 0.01 g. Seven blood samples were collected from jugular veins at −0.94, +5.26, +29.04, +53.24, +76.99, +101.16 and +125.17 h (SD = 0.17 to 0.40 h) relative to D_2O injection. Blood samples were drawn into tubes containing clot activator (BD Medical, Le Pont-de-Claix, France) *via* venipuncture, allowed to clot overnight at +4 °C, and serum was separated by centrifugation at 2000×g for 15 min at 4 °C, and stored at −20 °C until analysis.

Serum samples were thawed at room temperature, and 1 mL was subjected to cryodistillation [14] to extract the serum water and

	Before D_2O injection		D_2O dilution period						At slaughter
Days relative to the D_2O injection	-2	-1	0	1	2	3	4	5	6 - 9
Body weight	x	x	x		x				x
Milk yield and composition			x	x	x	x	x	x	x
Blood sampling (D_2O)			x	x	x	x	x	x	x
Body condition score and measurements						x			
3D and ultrasound imaging						x			
Computer tomography									x
Bioelectrical impedance spectroscopy									x
Adipose cell size									x

Fig. 1. Timeline of measurements and procedures relative to the day of D_2O injection (day 0).

condense it into a collection tube. The water was evaporated by heating the sample in a water bath (65 °C) and then condensed by cooling with an ethanol/liquid nitrogen mixture (−50/−70 °C) for 60 min. Extracted water was then transferred to glass tubes sealed with butyl/polytetrafluoroethylene caps and stored at 4 °C, followed by analysis for $^2H/^1H$ enrichment by IRMS at SILVATECH within a week (INRAE, 2018. Structural and Functional Analysis of Tree and Wood Facility, https://doi.org/10.15454/1.5572400113627854E12). Isotope ratios of $^2H/^1H$ were measured using a continuous flow EuroPyrOH (EuroVector, Milano, Italy) coupled, *via* a gas box interface, to an Isoprime isotope ratio mass spectrometer (IRMS, Elementar, Manchester, UK). The water was sampled by a 1-µL syringe. The autosampler HT300A (EuroVector) injected 0.2 µL into a quartz tube filled with Cr powder and heated to 1020 °C. The Cr reduces to H_2 ($^1H_2$, mass 2) and HD (^1H ^2H, mass 3) gases. The helium gas was used to carry H_2 or HD from the EuroPyrOH to the IRMS. Three international standards [Enriched Water (IAEA-604); Vienna Standard Mean Ocean Water (VSMOW); Greenland Ice Sheet Precipitation (GISP)] from the International Atomic Energy Agency (Vienna, Austria) were used to analyze samples. The results were expressed as delta values (‰) relative to VSMOW.

Parameters of D_2O dilution kinetics were computed for each goat by extrapolating the regression of the D_2O concentrations (C_t) over time, using the following equation: $C_t = C_0 \times \exp^{-k \times t}$ in which C_0 (intercept) is the theoretical D_2O concentration at injection (t = 0), k (slope) is the water turnover, and t is the time elapsed since D_2O administration [15,16]. Deuterium oxide C_0 and background concentration (C_{bg}, before D_2O injection) were then used to calculate the D_2OS in kg by using the equation from Schoeller et al. [17]:

$D_2OS = (Q_{D2O} \times APE_{dose} \times MW_{H20})/[MW_{dose} \times 100 \times (C_0 - C_{bg}) \times R_{std}]$,where Q_{D2O} is the dose of D_2O administered in grams, APE_{dose} is the deuterium atomic enrichment of the dose in percentage (i.e., 99.97%), MW_{H20} is the molecular weight of the body water (H_2O: 18.02 $g.mol^{-1}$), MW_{dose} is the molecular weight of D_2O (i.e., 20.02 $g.mol^{-1}$), C_0 and C_{bg} are expressed as delta ^2H *vs.* VSMOW (‰), and R_{std} is the ratio of deuterium to hydrogen in VSMOW (i.e., ^2H to ^1H ratio, 1.5576×10^{-4}).

2.2.3. Three-dimension imaging

Three-dimension images of goats were acquired at day 3 of the experiment using two devices, i) a portable system (Camera sensor Primesense Carmine / ASUSTek Computer Inc., Taipei City, Taiwan) was used to estimate BCS from images captured at the lumbar and pelvic locations [18], and ii) a fixed system Morpho 3D [19] was used to capture the body shape of the whole animal.

The portable system capture two pictures by a single sensor at approximately 60 cm from the animal's pelvic and lumbar areas to generate 3D images where 4 anatomical locations are positioned (Supplementary file S1). The coordinates (on axis X, Y and Z) of these 4 anatomical locations were used to estimate lumbar and sternal BCS [18].

The 3D image scanner Morpho 3D was previously described by Le Cozler et al. [19] and had only been used in dairy cows until now. Briefly, the device includes a total of 5 cameras in combination with an infrared laser projector (650 nm laser) installed on a mobile portal that scans the animal moving from the caudal to the cranial extremity of the animal, before returning to its initial position. Image capture (80 images per second) of the laser stripes projected onto the goat was used for 3D reconstruction of the entire animal. After a cleaning process and application of Poisson surface reconstruction algorithm, final 3D image was available for analysis. This technology was validated for linear measurements, circumferences, volumes and surfaces on dairy cows [19,20]. Total body volume and surface as well as five body dimensional measurements were obtained from image analyzes. These linear measurements correspond to chest depth, body length and chest girth measured at three locations, as described in Section 2.2.1. and in the Supplementary S1 file.

2.2.4. Ultrasound imaging

At day 3 of the experiment, ultrasound measurements were performed using an Aloka Prosound 2 unit equipped with a 5 MHz linear probe (UST5820-5; Hitachi Medical Systems SAS, F-69800 Saint-Priest, France). Measurements were made at lumbar and sternal areas using identifiable anatomical features, such as bone and cartilage, as reference locations. At the lumbar area, the probe was positioned parallel to the lumbar vertebrae (L2 and L3) at approximatively 1 cm of the spinous process to measure the thickness of subcutaneous adipose tissue and muscle. At the sternal area, the probe was positioned over the sternum. Ultrasound measurements at this site do not allow to distinguish measurements of skin and adipose tissue thickness. The same experienced operator scanned, interpreted all the images and performed all measurements. The anatomical locations and position of the probe are presented in the Supplementary S1 file.

2.2.5. Computer tomography

Goats were milked and weighed before the transport to the slaughterhouse (from d 6 to 9) where they were anesthetized by ketamine (100 mg/mL; 0.05 mL/kg BW i.v.; Imalgene 1000, Merial, Lyon, France) before CT measurements. Animals were placed on an inflatable mattress (Corben, Le Havre, France) to ensure minimal movements during CT acquisition. The CT acquisition was performed with a Siemens emotion duo CT scanner (Siemens, Erlangen, Germany) with the following acquisition parameters: tube tension 130 kV, tube current 40 mAs, slice thickness 3 mm, FoV 500 mm × 500 mm, matrix 512 × 512, convolution kernel B30s (soft tissue). Between 400 and 500 images were generated per goat. Image analysis was performed in three different steps. The first step was to separate goat images from images of their collars, CT table, and parts of the mattress by binarization, connected component labeling and by keeping the largest label functions of the MorphoLibJ plugin [21] for the ImageJ software [22]. Remaining inaccurate voxels were removed manually. The second step

was to separate the omasum and rumen semi-automatically from the image using turtleseg software (www.turtleseg.org; [23,24]). The third step was to perform the segmentation of fatty tissue, soft tissue and bone by automatic thresholding based on Hounsfield units (HU) on the CT images. Voxels ranging between −500 and −1 HU were classified as fatty tissue, voxels ranging between 0 and 120 HU were classified as soft tissue and voxels above 121 Hu were considered as bone. The automatic segmentation was performed using an in-house image analysis software [25]. Soft tissue, fatty tissue and bone volumes were available for entire goat image sets excluding rumen and omasum.

2.2.6. Bioelectrical impedance spectroscopy

Bioelectrical impedance spectroscopy was performed using ImpediVet Bioimpedance Spectroscopy device (ImpediMed Limited, Brisbane, Australia). Immediately after the CT-Scan, anesthetized goats were laid on the left flank on an isolated mat. Four needles (18G, 40 mm, BD Microlance, becton, Dickinson and Co, Plymouth, UK) were used as electrodes and were inserted subcutaneously and further attached to the BIS-electrodes. The two current electrodes were placed middle height on the hind leg, 5 cm cranially from the body end, and 5 cm caudal of the right scapular spine. The corresponding voltage-sensing electrodes were placed 5 cm on the same horizontal axis between the current electrodes (configuration 1 in Schäff et al. [9], see Supplementary S1 file). Hair on the right hind leg and caudal of the scapular spine was trimmed the day before BIS measurements.

The distance (L) between voltage-sensing electrodes was measured. Five continuous BIS measurements (1 measurement/s) were acquired from 4 kHz to 1 MHz (scans of 256 frequencies). The acquired data were downloaded and analyzed using complex impedance plotting with the ImpediVet BIS software (version 1.0.0.4) to determine body resistance at zero frequency (R_0), infinite frequency (R_∞), at 50 kHz (R_{50}) and 500 kHz (R_{500}), and body reactance at 50 and 500 kHz (Xc_{50} and Xc_{500}, respectively), based on the mean of the 5 BIS measurements. Other variates computed from L and those five BIS single measurements are reported in Supplementary Table S1.

Two goats were excluded from the BIS dataset due to technical problems and aberrant measurements.

2.2.7. Adipose cell diameter

Immediately after slaughter (Section 2.3, Fig. 1), approximately 100 mg of sternal and perirenal adipose tissue samples were collected, placed in a physiological saline solution at 37 °C and fixed in osmium tetroxide within 30 min following collection, as previously described [5]. After two weeks at room temperature, adipose cells were isolated in an 8 M urea solution, and the diameter of approximately 300 adipocytes was determined microscopically using Visilog software (version 6.7, Visilog software, Thermo Fischer Scientific, Waltham, Massachusetts, USA). Two goats were excluded from the ACD dataset due to technical problems. These goats were not the same as the ones excluded for BIS.

2.3. Slaughter and direct body composition measurements by chemical analyzes

Slaughter was performed on 4 successive days (from day 6 to 9 relative to D_2O injection, 4 to 6 goats per day) at the "Unité Expérimentale Porcs de Rennes" (INRAE, PR, 35590, Saint-Gilles, France). Immediately after CT and BIS measurements (see Sections 2.2.5 and 2.2.6), anesthetized goats were slaughtered by electronarcosis followed by exsanguination. Blood, perirenal adipose tissue and full total digestive tract were collected and weighed separately. The full total digestive tract was separated into five approximate sections (reticulo-rumen, omasum, abomasum, small and large intestine) that were sealed and weighed before and after emptying, in order to determine organ and content weights. The water content of each section was measured by desiccation of digesta samples at 103 °C for 48 h to estimate total digesta and water mass.

Skin, head, horns and lower legs were removed, combined and weighed. Abdominal and thoracic organs, visceral adipose tissue depots, empty digestive tract were combined and weighed. The carcass was divided into two halves (left and right) and weighed. The left half carcass and remaining EB parts (i.e., blood, skin, head, lower legs, internal organs, empty digestive tract, visceral adipose tissues) were stored at −20 °C in hermetic plastic bags before grinding. Each bag was weighed before freezing and after removal from storage, any weight loss was assumed to be water. Frozen left half carcass and remaining EB components were processed separately through mincing, mixing and homogenization using an industrial flaker (Rotary Meat Flaker, model RF15; Hobart, Cesson-Sévigné, France) to decrease the size of frozen blocks, followed by grinding and homogenization using an industrial-grinder (Mixer-grinder, model 4346; Hobart, Cesson-Sévigné, France). Three 250 g samples of homogenized carcass and remaining EB components were stored at −20 °C. Two samples were later thawed at 4 °C for 24 h, mixed with Fontainebleau sand (Dutscher, Brumath, France), and desiccated at 103 °C for 24 h to determine dry matter content. The third sample was lyophilized and finely ground with liquid nitrogen using a knife mill (Grindomix GM200, Retsch, Haan, Germany) before chemical analyses in duplicate: residual dry matter (desiccation at 105 °C for 3 h), lipid (ISO 6492:1999, petroleum ether extraction with a Büchi Speed Extractor E-916, Flawil, Switzerland), protein (ISO 16634-1:2008, N × 6.25 by Dumas combustion – thermal conductivity with a Leco Trumac CNS, St. Joseph, Michigan, USA), mineral (ISO 5984:2002, 550 °C until constant weight) and energy content (expressed as Mcal, 1 Mcal is equivalent to 4.184MJ; ISO 9831:1998, adiabatic calorimetry with an oxygen bomb calorimeter, IKA model C200, Fondis Bioritech, Guyancourt, France) were performed. Intra-assay coefficient of variation (CV) for carcass and remaining EB component samples were 0.48 and 0.93% for dry matter, 1.15 and 1.11% for lipid, 0.63 and 0.68% for protein, 2.9 and 8.2% for mineral, and 0.71 and 0.70% for energy, respectively. Full carcass composition was calculated by weighing the composition of left half carcass relative to total carcass weight, assuming an equivalent chemical composition of both half carcasses. Mass of EB water, lipid, protein, minerals and energy was computed from the sum of whole carcass and remaining EB parts. Total body water mass was further computed as the sum of EB water and digesta water.

2.4. Statistical analyses

Correlations, simple and multiple regressions were performed using the CORR and GLM procedures of SAS 9.4 (SAS Inst. Inc., Cary, NC) to evaluate relationships among different variates, and develop estimation equations of EB composition from predictive variates derived from the eight tested methods. Simple regressions between EB composition and predictive variates were explored by offering one variate at a time. Then, multiple regressions were tested by offering BW and additional predictive variates using a stepwise approach, separately for each of the eight methods studied. Significance was predefined as $P \leq 0.05$, and trends toward significance at $0.05 < P \leq 0.10$. Fitness of regression models were assessed by residual plot analyses, R^2 and residual standard deviation (rSD).

3. Results

3.1. Body composition measured after slaughter

The sum of analyzed body components (*post-mortem* BW) was close to the BW recorded before slaughter (Table 2). The unaccounted loss of material averaged 1.8% and was always lower than 5% of pre-slaughter BW. Body weight changed +0.4% on average (from −5% to +6%) during the experimental period. The BW at slaughter was 54.7 ± 6.6 kg (mean ± SD, range 45.6 to 66.9 kg). Digesta mass

Table 2
Anatomical measurements and chemical composition measured after slaughter of dairy goats (n = 20).

Item[1]	Mean	SD	Min	Max
Anatomical measurements (kg)				
D_2O infusion BW[2]	55.1	7.5	45.8	69.3
Ultrasound and 3D imaging BW[3]	54.1	7.1	45.2	69.0
Pre-slaughter BW[4]	54.7	6.6	45.6	66.9
Post-mortem BW[4]	53.7	6.4	45.4	65.9
Digesta content	15.4	2.4	10.5	20.4
EB weight	38.2	6.2	31.5	51.7
Perirenal adipose tissue weight (kg)	0.399	0.367	0.045	1.452
Chemical composition (kg)				
Total body water	38.6	3.8	32.3	46.2
Digesta water	13.6	2.2	8.9	17.8
EB water	25.0	3.0	21.3	31.5
EB lipid	4.5	2.7	0.8	9.9
EB protein	6.7	0.9	5.8	8.6
EB mineral	1.9	0.3	1.6	2.4
Fat-free EB	33.7	4.0	28.8	42.4
EB energy (Mcal)[5]	80	30	41	141
Proportions of body components in EB weight (%)				
Water	65.8	4.5	57.4	75.2
Lipid	11.2	5.1	2.1	20.4
Protein	17.7	0.7	16.3	18.9
Minerals	5.1	0.4	4.3	5.8
Energy (Mcal/kg)[5]	2.05	0.46	1.14	2.87
Proportions of body components in fat-free EB weight (%)				
Water	74.1	1.0	72.1	76.9
Protein	20.0	0.7	17.8	21.5
Minerals	5.8	0.4	5.1	6.6

[1] BW: body weight, EB: empty body.
[2] Day 1 of the experiment.
[3] Day 3 of the experiment.
[4] Days 6 to 9 of the experiment corresponding to computer tomography, impedancemetry and adipose cell size measurements. Pre slaughter BW corresponds to the live weight measured the morning before slaughter, *post-mortem* BW corresponds to the sum of all body compartments collected after slaughter.
[5] One Mcal is equivalent to 4.184 MJ.

corresponded to 29.0 ± 4.5% and EB to 71.0 ± 4.5% of BW at slaughter. Total body water averaged 38.6 ± 3.8 kg, among which 35.2 ± 4.3% was digesta water and 64.8 ± 4.3% was EB water. Empty body water ranged from 21.3 to 31.5 kg and corresponded to 57.4 to 75.2% of EB weight. A comparable variability in EB was observed for lipid (0.8 to 9.9 kg, 2.1 to 20.4%) and energy (41 to 141 Mcal, 1.14 to 2.87 Mcal/kg), whereas protein (5.8 to 8.6 kg, 16.3 to 18.9%) and mineral (1.6 to 2.4 kg, 4.3 to 5.8%), were less variable.

When reported on fat-free EB (EB – EB lipid mass), percentages of water, protein and mineral were fairly constant among the 20 goats (e.g., 72.1 to 76.9% of water, Table 2). Accordingly, water and lipid expressed as percentage of EB were closely and negatively related ($P < 0.001$, Fig. 2), with the following equation:

The equation Lipid (% EB weight) = −1.12 (± SE = 0.03) × water (% EB) + 85.17 (± 2.24) and residual SD (rSD) = 0.66 %, residual coefficient of variation (rCV) = 5.9 %, R^2 = 0.984, n = 20.

3.2. Variates derived from the eight tested methods

Measurements from the eight methods used for the estimation of body composition are presented in Table 3. Chest depth varied from 34 to 44 cm, with a CV of 8%, higher than the CV of height-at-withers (3%) and the heart girth at the withers (5%). The chest depth and the heart girth measurements performed using the whole animal 3D imaging scan method were only slightly correlated with the same measurements performed manually (r = +0.35 and +0.55, respectively). Nonetheless, their means were close between the two techniques (−5% and +7% between 3D and manual measurements for chest depth and

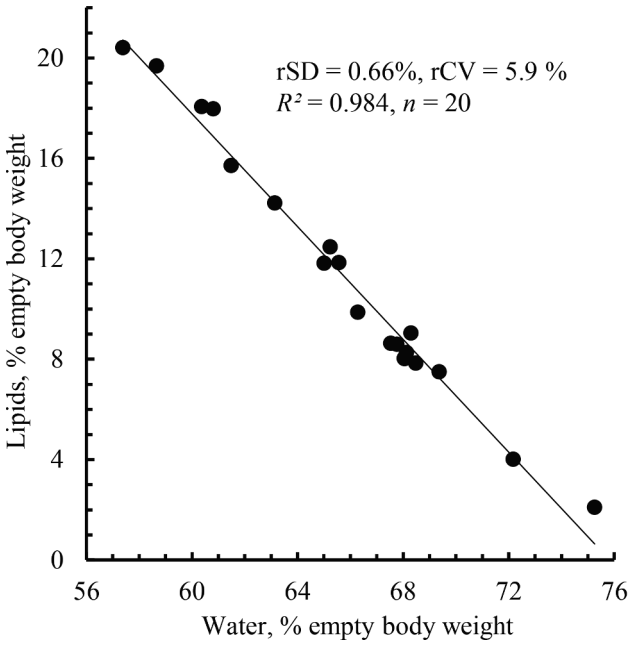

Fig. 2. Relationship between empty body water and lipid content of dairy goats.

Table 3
Main measurements derived from the tested techniques for estimation of body composition of dairy goats (n = 20).

Item	Mean	SD	Min	Max
Morphological measurements (cm)				
Height at withers	73	2	69	77
Heart girth	87	4	82	95
Maximum chest depth[1]	39	3	34	44
D_2O dilution space (kg)	41.9	4.5	34.9	52.4
Bioelectrical impedance spectroscopy[2]				
R_0 (Ω)	61.9	5.2	51.8	69.9
R_∞ (Ω)	27.8	2.7	22.2	32.8
L^2 / R_0 (cm^2/Ω)	74.4	10.1	58.4	92.4
L^2 / R_∞ (cm^2/Ω)	166.1	21.6	133.5	216.3
Adipose cell size (μm)				
Perirenal	76	18	48	111
Sternal	67	9	50	85
Body condition score (BCS, 0–5)				
Lumbar	2.5	0.4	1.8	3.0
Sternal	2.6	0.5	1.8	3.3
BCS estimate from 3D imaging (0–5)				
Lumbar	2.5	0.4	1.6	3.2
Sternal	2.8	0.6	1.7	3.8
Ultrasounds thickness (cm)				
Lumbar muscle	2.4	0.4	1.9	3.8
Sternal muscle	2.5	0.7	1.5	4.1
Lumbar adipose tissue	0.23	0.04	0.18	0.35
Whole body 3D imaging technique				
Total body volume (L)	67	7.0	53.1	80.7
Total body surface (m^2)	1.74	0.16	1.46	2.04
Computer tomography (L)				
Total body volume	56.6	6.7	47.5	68.9
Fatty tissue volume	9.3	3.2	5.0	17.0
Soft tissue volume	18.6	2.5	13.0	24.5
Bone volume	2.9	0.4	2.4	3.8

[1] Measurement was performed at the abdominal region (see supplementary file 1 for details).
[2] R_0: Body resistance at zero frequency, R_∞: Body resistance at infinite frequency, L^2: square of the distance between measuring electrodes.

hearth girth, respectively). The 3D-scan method provided automatic estimates of total body surface and volume. The latter was slightly correlated with the total body volume estimated by the CT method (r = +0.39), with an average overestimation for 3D scan of +18%.

Among the body tissue volumes estimated by CT, 'fatty tissues' was the most variable (CV: 34%), followed by 'bones' (14%), 'soft tissues' (13%) and total volume (12%).

Body condition score estimated either by palpation or 3D imaging presented high correlation at both the lumbar (r = +0.67) and sternal (r = +0.71) locations and provided similar values (Table 3). Body condition score was variable among the 20 goats selected for this study (CV of 15 to 28%), for both manual and 3D methods. A similar variability was observed for the thickness of lumbar and sternal muscles estimated by the US method (2.4 and 2.5 cm, and CV of 17 and 28% for lumbar and sternal muscles, respectively), and for the perirenal and sternal adipose cell size (76 and 67 μm, CV of 24 and 13%, respectively). The variability was low for R_0 and R_∞ measured by the BIS method (means of 61.9 and 27.8 Ω, CV of 8 and 9%), and for the D_2OS approach (41.9 kg and CV of 11%).

Total body water at the time of D_2O injection was calculated as total body water at slaughter + (BW at D_2O injection − BW at slaughter) × digesta water proportion (%) measured at slaughter, assuming that BW differences between the day of D_2O injection and slaughter were due to changes in digesta mass. The relationship between total body water estimated at the time of D_2O injection and the D_2OS was precise (Fig. 3) and is defined by the following equation:

Total body water at the time of D_2O injection (kg) = 1.076 (± 0.081) × D_2OS (kg) − 6.222 (± 3.402); rSD = 1.57 kg, rCV = 4.0%, R^2 = 0.908, n = 20, P < 0.001 and P = 0.08 for slope and intercept, respectively.

3.3. Estimation of EB of chemical components mass

Table 4 reports the most precise multiple linear regression equations for the estimation of EB water, lipid, protein and mineral mass, and EB energy content using BW and independent variates derived from the eight methods tested. Supplementary Table S2 presents simple linear regressions for the estimation of EB chemical component mass. Plots of residuals for the best equations are illustrated in Fig. 4 for EB lipid mass, and in Supplementary Figs. S1 and S2 for EB protein mass and EB energy, respectively.

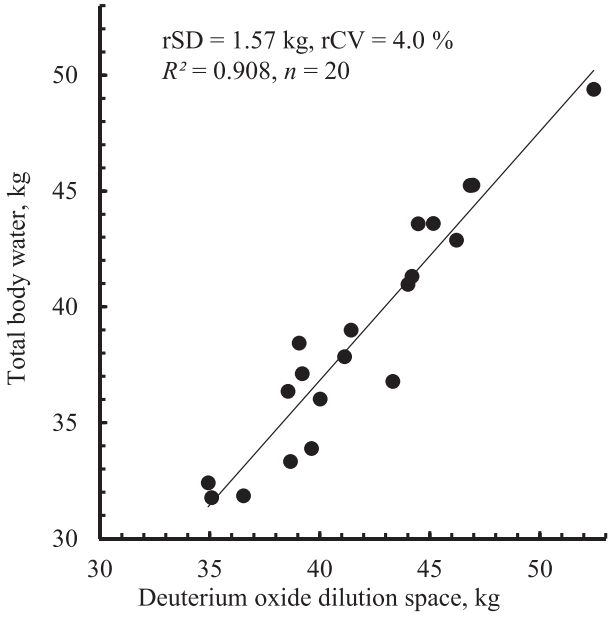

Fig. 3. Relationship between deuterium oxide dilution space and total body water of dairy goats.

3.3.1. Water

Body weight alone provided a fair estimate of EB water mass (R^2 = 0.80), a relationship which was improved (P < 0.01) when D_2OS was added (R^2 = 0.91, Table 4). Only total body volume measured by CT was a better single predictor of EB water (R^2 = 0.87, Supplementary Table S2) compared to BW alone.

3.3.2. Lipid and energy

For single regression equations, BW alone did not provide a good estimate of EB lipid mass (R^2 = 0.60) or EB energy (R^2 = 0.67, Table 4). The best single estimators of EB lipid mass and EB energy in descending order of R^2 were: i) volume of fatty tissues measured by CT (R^2 = 0.92 and 0.94), ii) perirenal adipose tissue mass (R^2 = 0.82 and 0.82), iii) cell diameter (R^2 = 0.83 and 0.78), iv) sternal BCS recorded manually (R^2 = 0.75 and 0.73), v) R_∞ measured by BIS (R^2 = 0.67 for EB lipid), and vi) lumbar BCS recorded manually (R^2 = 0.64 for EB lipid). At the exception of the volume of fatty tissues measured by CT, the R^2 of all of the single regression relationships increased when BW was added as a second independent variate in multiple regression. Thus, the best multiple regression equations, in descending R^2 order, were obtained by combining BW with i) perirenal adipose tissue mass and cell diameter (R^2 ≥ 0.95), ii) D_2OS (R^2 ≥ 0.91) and iii) R_∞ measured by BIS (R^2 ≥ 0.87). Sternal BCS recorded manually combined with either BW or heart girth also provided good equations for EB lipid (R^2 = 0.80 and 0.81 for BW and heart girth, respectively) and EB energy (R^2 ≥ 0.82). Lumbar BCS recorded using 3D imaging method combined with BW provided slightly lower R^2 for EB lipid mass (R^2 = 0.74) and EB energy (R^2 = 0.77, Table 4, Fig. 4 and Supplementary Fig. S2). Conversely, variates derived from sternal ACD, ultrasound and whole body 3D imaging methods were not satisfactory estimators of EB lipid mass nor EB energy, when included alone or combined with BW in linear regressions (R^2 ≤ 0.40 and 0.27 for US and whole body 3D imaging, respectively, Supplementary Table S2).

3.3.3. Protein and minerals

Body weight alone explained 92% and 72% of the variance of EB protein and mineral mass, respectively (Table 4). The BW was superior to all other single independent variates tested in our study. Only total body volume measured by CT (R^2 ≥ 0.70) and heart girth recorded manually (R^2 ≥ 0.64) explained more than 50% of the variance in protein and mineral mass, and D_2OS presented a R^2 of 0.60 for EB protein mass (Supplementary Table S2).

For EB protein mass, multiple regressions including BW associated with either D_2OS (R^2 = 0.97), sternal BCS recorded manually or heart girth (R^2 = 0.95) improved the R^2 compared to the simple BW regression (Table 4 and Supplementary Fig. S1). For EB mineral mass, multiple regressions including BW with soft tissue volume measured by CT (R^2 = 0.77) or BW with thickness of the lumbar muscle measured by US (R^2 = 0.75) improved the R^2 compared to the simple BW regression (Table 4).

3.4. Estimation of EB chemical component percentage

The most precise multiple linear regression equations estimating the percentage of EB water, lipid, protein, mineral and energy are reported in Supplementary Table S3. Overall, a lower R^2 was observed for the estimation of EB percentages compared to mass estimation, except for EB water and EB protein by BIS measurements (R^2 ≥ 0.54 *vs.* R^2 ≥ 0.32), and for EB water estimation by sternal BCS recorded manually (R^2 = 0.74 *vs.* 0.23; Supplementary Tables S2 and S3). Body weight alone was not a good estimator of EB percentage of water (R^2 = 0.38), lipid (R^2 = 0.43), protein (R^2 = 0.36), mineral (R^2 = 0.24) or energy (R^2 = 0.41). Three methods allowed to explain

Table 4
Most precise estimation equations predicting empty body chemical component mass measured after slaughter using body weight and independent variates derived from each tested method[1].

Chemical component		Statistics		
Methods	Equations [mean (SE)][2]	rSD	rCV (%)	R^2
Water (kg)				
Body weight	0.403 (0.047) × BW + 2.894 (2.596)	1.347	5.4	0.803
D_2O dilution space	0.272 (0.073) × BW + 0.239 (0.107) × D_2OS + 0.095 (2.660)	0.951	3.8	0.907
Computer tomography	0.410 (0.038) × CT total vol + 1.765 (2.164)	1.109	4.4	0.866
Lipids (kg)				
Body weight	0.316 (0.061) × BW − 12.800 (3.364)*	1.745	38.7	0.598
D_2O dilution space	0.698 (0.057) × BW − 0.833 (0.095) × D_2OS + 0.966 (1.882)	0.848	18.8	0.911
Bioelectrical impedance spectroscopy	0.209 (0.045) × BW + 0.591 (0.109) × R_∞ − 23.252 (2.877)*	1.085	23.2	0.865
Adipose cell diameter	0.103 (0.029) × BW + 0.069 (0.017) × perirenal ACD + 1.782 (0.819) × perirenal AT weight − 6.779 (1.798)*	0.567	11.6	0.954
Body condition score	0.106 (0.050) × BW + 4.007 (0.759) × sternal BCS − 11.782 (2.274)*	1.273	28.2	0.798
	4.231 (0.667) × sternal BCS + 0.219 (0.090) × heart girth − 25.698 (7.246)*	1.232	27.4	0.811
Body condition score by 3D imaging	0.202 (0.049) × BW + 4.042 (0.972) × lumbar 3D BCS − 16.337 (3.050)*	1.456	32.3	0.740
Computer tomography	0.811 (0.055) × CT fat vol − 3.033 (0.536)*	0.758	16.8	0.924
Proteins (kg)				
Body weight	0.130 (0.009) × BW − 0.362 (0.489)	0.254	3.8	0.922
D_2O dilution space	0.158 (0.011) × BW − 0.082 (0.019) × D_2OS + 1.481 (0.376)*	0.169	2.5	0.967
Body condition score	0.056 (0.018) × BW + 0.429 (0.135) × sternal BCS + 0.103 (0.034) × heart girth − 6.390 (2.221)*	0.219	3.3	0.948
Minerals (kg)				
Body weight	0.033 (0.005) × BW + 0.160 (0.265)	0.138	7.1	0.717
Ultrasounds	0.027 (0.006) × BW + 0.130 (0.087) × US lumbar muscle + 0.146 (0.257)	0.133	6.9	0.750
Computer tomography	0.043 (0.007) × BW − 0.035 (0.018) × CT soft vol + 0.242 (0.251)	0.128	6.6	0.768
Energy (Mcal)[3]				
Body weight	3.73 (0.61) × BW − 123.96 (33.76)*	17.51	21.8	0.673
D_2O dilution space	7.58 (0.56) × BW − 8.48 (0.93) × D_2OS + 17.99 (18.36)	8.27	10.3	0.931
Bioelectrical impedance spectroscopy	2.69 (0.46) × BW + 5.86 (1.12) × R_∞ − 228.61 (29.61)*	11.17	13.6	0.885
Adipose cell diameter	1.56 (0.27) × BW + 0.60 (0.15) × perirenal ACD + 22.04 (7.59) × perirenal AT weight − 54.47 (16.66)*	5.25	6.2	0.968
Body condition score	1.59 (0.52) × BW + 40.25 (7.92) × sternal BCS − 111.80 (23.75)*	13.29	16.6	0.822
	44.16 (6.97) × sternal BCS + 3.12 (0.94) × heart girth − 307.46 (75.71)*	12.88	16.0	0.833
Body condition score by 3D imaging	2.55 (0.50) × BW + 40.42 (10.10) × lumbar 3D BCS − 157.22 (31.71)*	15.13	18.9	0.770
Computer tomography	9.08 (0.56) × CT fat vol − 4.18 (5.46)	7.72	9.6	0.937

*indicates that intercept is significantly different from 0 ($P < 0.05$).

[1] Body weight (BW) used in the regression equations was recorded the closest to the measurement of each method: Pre slaughter BW for BW alone, biolectrical impedance spectroscopy, adipose cell diameter and computer tomography methods; morning BW on the day of 3D imaging, ultrasound and body condition score methods; and BW at the time of D_2O injection for D_2O dilution space method.

[2] Abreviations and units: BW: body weight (kg), D_2OS: D_2O dilution space (kg), CT total vol: total body volume measured by computer tomography (L), R_∞: body resistance at infinite frequency measured by bioelectrical impedance spectroscopy (Ω), perirenal ACD: perirenal adipocyte cell diameter (μm), perirenal AT weight: weight of perirenal adipose tissue (kg), sternal BCS: body condition score at the sternal location (0–5 scale), Heart girth: chest round size at the withers location (cm), lumbar 3D BCS: body condition score at the lumbar location estimated by 3D imaging method (0–5 scale), CT fat vol: volume of fat tissues measured by computer tomography (L), CT soft vol: volume of soft tissues measured by computer tomography (L), US lumbar muscle: thickness of the lumbar muscle measured by ultrasounds (cm).

[3] One Mcal is equivalent to 4.184 MJ.

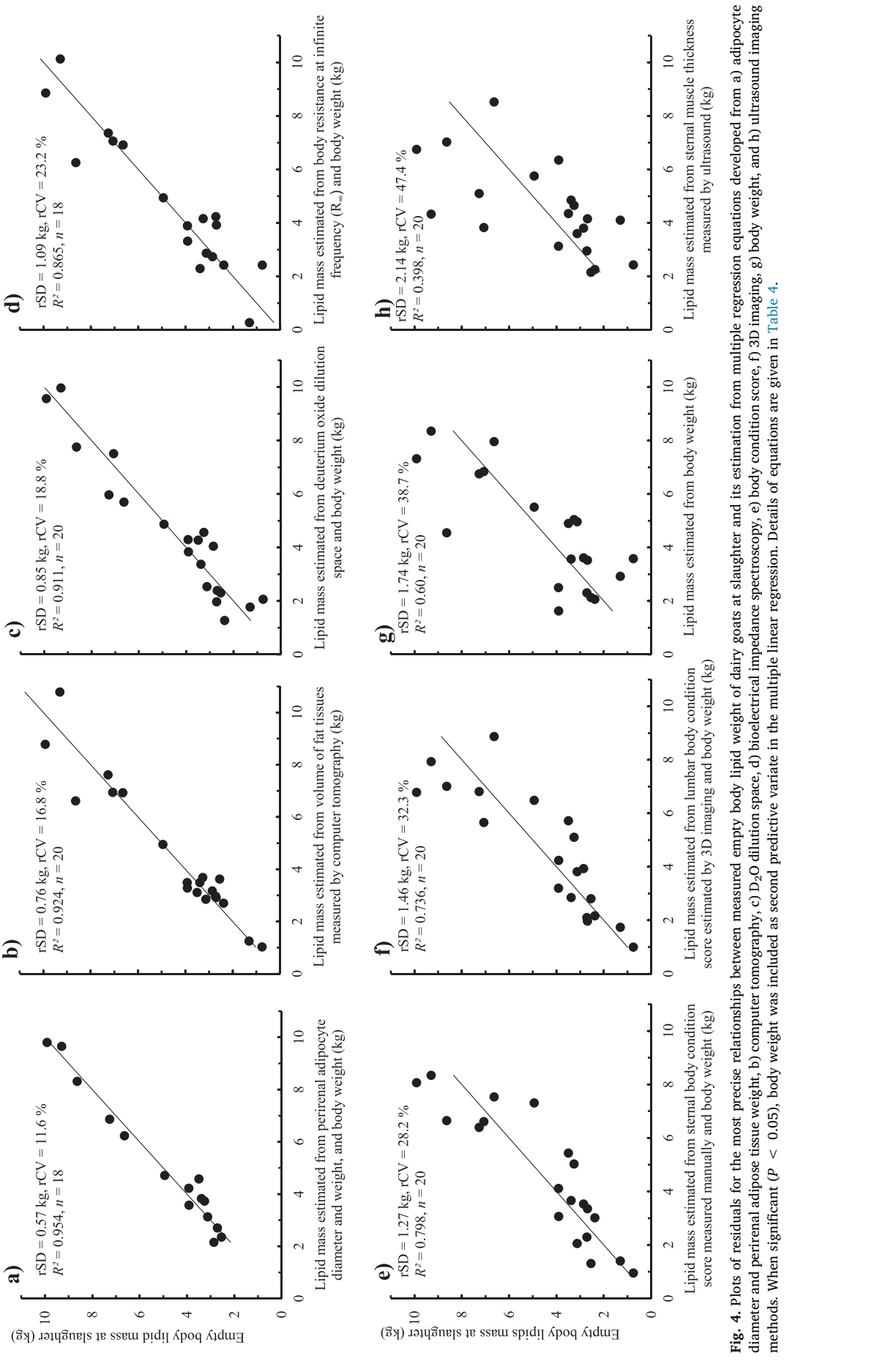

Fig. 4. Plots of residuals for the most precise relationships between measured empty body lipid weight of dairy goats at slaughter and its estimation from multiple regression equations developed from a) adipocyte diameter and perirenal adipose tissue weight, b) computer tomography, c) D_2O dilution space, d) bioelectrical impedance spectroscopy, e) body condition score, f) 3D imaging, g) body weight, and h) ultrasound imaging methods. When significant ($P < 0.05$), body weight was included as second predictive variate in the multiple linear regression. Details of equations are given in Table 4.

at least 80% of the variance of EB percentage of water, lipid and energy. The most precise methods were the measure of perirenal ACD (R^2 > 0.86), followed by fatty tissue volume as percent of total volume measured by CT (R^2 ≥ 0.86), D_2OS per kg BW (R^2 ≥ 0.80), and sternal BCS recorded manually (R^2 ≥ 0.74). Equations combining BW with R_∞ measured by BIS, and BW with lumbar BCS recorded by 3D imaging method explained between 70 and 80% of the variance (Supplementary Table S3). Conversely, variates derived from 3D whole body scan and US failed to estimate EB water, lipid or energy percentage (R^2 ≤ 0.42).

For EB protein percent, only perirenal ACD (R^2 = 0.79), D_2OS per kg BW (R^2 = 0.70), R_∞ measured by BIS (R^2 = 0.54) and lumbar BCS recorded manually (R^2 = 0.53) explained more than 50% of the variance. In the case of EB mineral content, none of variates derived from the eight methods were able to explain more than 50% of the variance, either alone or with BW as a second variate in multiple regression (Supplementary Table S3).

4. Discussion

This study compared eight methods for *in vivo* estimation of body composition, through their respective calibration against chemical composition measured *post-mortem*. We compared well-documented and established methods (i.e., D_2OS, BIS, ACD, BCS and US), and innovative approaches for which direct calibration is scarce or non-existent in the literature for dairy goats (i.e., 3D imaging and CT).

4.1. Body composition measured after slaughter

Empty body lipid percentage (11%; Table 2) was slightly lower than observed in previous direct *post-mortem* measurements of EB composition in lactating and dry goats (15 to 25%; [12,26–29]). This difference is explained by the exclusion of extremely fat goats in our study (up to 20% of EB lipids), whereas previous studies enrolled goats with up to 38% of EB lipids [27,28]. In the present study, we chose to assess the precision of the methods for estimation of body composition over a range commonly found in dairy goat operations, where fat goats are seldom present.

Percentages of water, protein and minerals in fat-free EB were almost constant (72 to 77%, 18 to 22% and 5 to 7%, respectively, Table 2), in accordance with previous studies (76 to 77% water, 19 to 21% protein, and 4 to 5% minerals in fat-free EB [27–29]). Consequently, EB lipid and water percentages were highly negatively correlated (r = −0.99, Fig. 2), as reported in previous studies (e.g., r = −0.98 to −0.96, [12,28,30]). Such constancy of the fat-free EB composition and the concomitant strong negative linear relationship between EB water and lipid percentages were expected and are well-established in animals [15,31].

4.2. Comparison of the precision of the eight methods tested for body composition estimation

The relative precision of the eight methods was established based on comparison of R^2 and rSD. Only R^2 is discussed because both indicators lead to similar ranking of methods.

As a single variate, BW explained 80 and 92% of the EB water and protein mass, respectively, but only 60 and 67% of EB lipid mass and EB energy, respectively (Table 4). Frequent measurements of BW, milk yield and composition allow to estimate energy balance of dairy cows [32,33]. Therefore, longitudinal monitoring of BW throughout lactation cycles may allow to assess relative changes of body composition for a given animal. However, in the present study, BW never explained more than 43% of the variance of EB chemical component percentages. These results confirm that BW alone rarely offers a precise estimate of the absolute ruminant EB composition [34], which may be explained by inter-individual size and anatomical differences (among and within breeds), the large percentage of digesta in the ruminant BW (28% in the present study), and its variability depending on diet and feeding behavior. Moreover, the relative percentage of EB tissues and organs change widely during growth, and gestation / lactation cycles due to body reserve mobilization and accretion [35].

In order to overcome the limitations of BW, many methods have been developed for *in vivo* estimation of livestock body composition over the past century. Four broad approaches were followed in order to estimate this key phenotypic trait: i) evaluation of external body shape and subcutaneous tissues; ii) measurement of volume or mass of internal tissues and organs; iii) measurement of the adipose cell size; and iv) quantification of body water mass.

Among the methods relying on the first principle (evaluation of external body shape and subcutaneous tissues), manual or 3D BCS, 3D whole body scan and US were compared. Manual BCS offered a good precision, especially the sternal BCS when combined with BW for estimations of EB lipid and EB energy (R^2 ≥ 0.80, Table 4). Similarly, Ngwa et al. [27] reported R^2 of 0.77 and 0.82 when estimating EB lipid and energy, respectively, from BW and BCS (combining lumbar and sternal locations); whereas sternal BCS estimated total adipose tissue mass (sum of omental, mesenteric, perirenal, subcutaneous and intermuscular) with a R^2 of 0.90 [11]. Manual BCS is a non-invasive method and does not require particular equipment, but is subjective and prone to operator bias. An automatic 3D-BCS method may mitigate these limitations. Compared to the manual sternal BCS, lumbar 3D-BCS combined with BW slightly decreased the precision of the predictive equation for EB lipid mass and EB energy (R^2 ≥ 0.74, Table 4). To the best of our knowledge, this is the first study exploring the relationships between EB composition measured after slaughter and 3D-BCS *in vivo*. A correlation of r = +0.50 was found between manual BCS and 3D-BCS using the same techniques in dairy goats [18], compared to r ≥ +0.67 in the present study.

The utilization of 3D imaging technology to acquire goat whole body shape failed to conveniently estimate body composition (R^2 ≤ 0.43, for all 3D whole scan measurements and EB chemical components, Supplementary Tables S2 and S3). The initial hypothesis was that 3D measurements of total body volume, area, or other specific body measurements would be good estimates of body composition. Indeed, the heart girth recorded manually offered a fair estimate of EB protein and minerals (R^2 = 0.83 and 0.64, respectively, Supplementary Table S2). However, a poor correlation was observed between hearth girth measured manually and by 3D body scan (r = +0.59). The tested 3D scan equipment was initially developed for cattle [19,20] and may be oversized to produce a precise 3D shape of small ruminants. To improve the performances of such 3D technology in goats, a dedicated smaller 3D scan equipment together with more complex and detailed exploitation of the 3D images, is necessary. Moreover, this technology was not initially developed to estimate body composition but to access to morphological traits, volumes, surfaces and estimated BW [19,20], with a high frequency of records on animals, from birth to slaughter and to analyze changes over time. Lastly, the US method failed to provide good predictive variates of body composition (R^2 ≤ 0.45), except for EB minerals, with a slight improvement of the regression when lumbar muscle thickness was combined with BW (R^2 = 0.75, Table 4). Conversely, in Blanca Celtiberica goats, the sternal adipose tissue thickness measured by US was a good estimator of total adipose tissue mass, when used alone (R^2 = 0.85, [11]) or in combination with BW (R^2 = 0.89, [36]). The current study did not include animals in the higher end of BCS (≤3.3). Ultrasonography failed to discriminate breed differences in subcutaneous adipose tissue mobilization in thin dairy cows [37]. The inclusion of fatter goats might have improved body composition predictions by US.

Computer tomography was chosen among imaging methods that measure tissue and organ volume. Tissue volume measured by CT was the most precise method for estimation of EB minerals (R^2 = 0.77), and the second most precise method for water, lipid, protein and energy (R^2 = 0.87, 0.92, 0.88 and 0.94, respectively, Table 4). Although CT

was recently employed for the assessment of body composition in goats [38,39], to our knowledge, only Sørensen [40] made a direct calibration of CT for estimation of body composition of Norwegian Landrace goats. This author reported a high precision of CT for estimation of EB lipid and energy (rSD = 4.5 *vs.* 7.7 Mcal in the present study for energy), and a slightly lower precision for EB water and protein mass, as observed in the present study. This high precision was expected, even though CT measurements of tissue volumes rather than mass of chemical components, and considering that both density and relative percentages of chemical components may vary within a specific group of tissues (fatty, soft or bone tissues). The main drawbacks of the CT method include requiring expensive equipment, anesthesia, specific skills and knowledge of ruminant anatomy, and time consuming post-acquisition image treatment [4].

Perirenal and sternal ACD was tested as a method to estimate EB lipid and other chemical components. Perirenal ACD combined with perirenal adipose tissue weight and BW was the most precise method for EB lipid and energy estimation ($R^2 \geq 0.95$, Table 4) among the eight methods evaluated. Nonetheless, sampling of perirenal adipose to measure ACD is highly invasive and difficult to perform on live animals. Conversely, sternal ACD can be determined *in vivo* by subcutaneous biopsy, but failed to precisely estimate EB composition ($R^2 \leq 0.33$). Indeed, previous studies in non-lactating Créole and Blanca Celtibérica goats reported low precision of sternal ACD to estimate total adipose tissue mass ($R^2 = 0.17$ and 0.44, [41,11], respectively). This discrepancy between adipose tissue depots (sternal and perirenal) may be explained by a late hyperplasia in the sternal adipose tissue in adult goats [35]. This hypothesis is supported by a bimodal distribution of ACD classes indicating hyperplasia that was observed in the sternal, but not in perirenal adipose tissues (data not shown). Indeed, the principle of relationship between ACD and EB lipid mass relies on the fact that body lipid dynamic should occur almost exclusively by changes in adipose cell size and not by hyperplasia in adult ruminants [35].

Deuterium oxide dilution space and BIS were tested, among methods that aim to quantifying body water. Deuterium oxide dilution space combined with BW was the most precise method to estimate EB water and protein mass ($R^2 \geq 0.91$), and the third for estimation of EB lipid and energy ($R^2 \geq 0.91$; Table 4). Similar precision was reported for the estimation of EB water (rSD ≤ 1.3 kg, [12,28]) and lipid (rSD ≤ 1.72 kg, [12,26,28,29]) from D_2OS or tritium water dilution space in lactating and dry goats. Such high precision was expected because i) water dilution space is a predictor of total body water ($R^2 \geq 0.91$, present study, [12,28]) and ii) there is a strong negative relationship between EB water and lipid percentages, as confirmed in the present study (see Section 4.1.) and elsewhere [12,28,30]. Deuterium oxide dilution space overestimated total body water by 8.8%, which is greater than the 1.0% overestimation reported by Schmidely et al. [12], but similar than the 11% recorded with tritium water method [28]. Such overestimation is often described, and is due to the exchange of deuterium or tritium with hydrogen atoms from organic matter molecules of EB and digesta [15,16]. The D_2OS technique is feasible in field studies, does not require specific equipment, and is moderately invasive (i.e. requires a series of blood samples over a few days), and does not impact animal behavior and performance significantly. Nonetheless, the time-consuming sampling and D_2O analyses (especially for blood water distillation), together with the costly IRMS equipment and required skills, limit its wider application for body composition phenotyping. Faster and cheaper alternatives for sampling matrices (e.g. milk rather than blood, [42]) and analytical procedures (e.g. use of centrifugal filtration tubes for water extraction rather than distillation [43], laser spectroscopy rather than IRMS [44]) may help to overcome these limitations but will require further methodological validation. Resistance at infinite frequency from BIS combined with BW was a slightly less precise method than D_2OS for the estimation of EB lipid and energy ($R^2 \geq 0.87$, Table 4), whereas BIS variates failed to estimate fairly EB water, protein and minerals ($R^2 \leq 0.42$). Similarly, a better relationship was obtained between goat kid carcass resistance at 50 kHz (R_{50}) and adipose tissue mass ($R^2 = 0.86$) compared to muscle mass ($R^2 = 0.38$, [45]). More complex measurements issued from BIS also provided good estimations of total adipose tissue mass ($R^2 \geq 0.96$) in dairy cows [9]. The BIS has the advantage of requiring a portable equipment, and providing immediate results without the need of sampling or laboratory analysis. Nonetheless, BIS may affect animal welfare because it requires subcutaneous insertion of electrode needles in precise anatomical locations and animals must be isolated from the ground for accurate and reproducible measurements [9].

5. Conclusions

This study compared eight methods for the estimation of EB composition using goats as a ruminant model. Overall, perirenal ACD method provided the best estimations of EB composition, especially for EB lipid and energy. Nonetheless, due to the limited feasibility of performing perirenal adipose tissue biopsies, this method may only be applied *post-mortem*. Concerning *in vivo* estimation of body composition, CT and D_2OS were both precise methods, but are time consuming and require expensive equipment and analyses. These disadvantages restrict the use of CT and D_2OS to animal research involving relatively low animal numbers. The BIS method was less precise than CT and D_2OS, but has the advantage of requiring small portable equipment, with no need of sampling and analyses, but may be invasive and sensitive to measurement error. Alternatively, manual BCS offered a satisfactory precision, is noninvasive, relatively fast, does not require equipment, and may be used on a large number of animals and on-farm. Nonetheless, manual BCS is subjective and prone to operator bias, a limitation that may be avoided by BCS assessment using 3D imaging techniques. However, in the present study, neither US nor whole body 3D imaging provided satisfactory estimators of EB composition. Further development and more complex measurements using 3D imaging could improve its precision. Ultimately, these may lead to the automatization of high-throughput phenotyping of body shape, with minimal disturbance of animal welfare. Longitudinal studies employing repeated automatic measurements of BW and 3D body shape may allow to phenotype accretion and utilization of body reserves and explore their contribution to individual robustness, with applications in animal research and precision livestock farming.

Acknowledgments

The authors thank A. Eveno, J.Y. Thébault, A. Chauvin, M. Texier-Quenouillère and the team of the “Installation Expérimentale en Production du Lait” of the UMR (INRAE, Méjusseaume, France) for diligent feeding, milking, management of goats and sample processing; J. Liger, J. F. Rouaud, and M. Alix (3P, INRAE, 2018. Pig Physiology and Phenotyping Experimental Facility, https://doi.org/10.15454/1.5573932732039927E12) for slaughter procedures and empty body mincing; N. Angeli, C. Hossann (INRAE, 2018. Structural and Functional Analysis of Tree and Wood Facility, https://doi.org/10.15454/1.5572400113627854E12) and A. Zahariev (IPHC, CNRS, Strasbourg, France) for D_2O analyses; S. Dubois and all the feed chemistry unit of Agroscope (Posieux, Switzerland); and I. Constant and M. Tourret (INRAE, UMR Herbivores, Saint-Genès-Champanelle, France) for empty body chemical analyses. Authors are grateful to M. Bonnet (INRAE, UMR Herbivores) for insightful advice leading to the genesis of the study.

Funding

This research was funded in part by the Department of Animal Physiology and Livestock Production Systems (PHASE) of INRAE, and the Join Technological Unit “Services rendus par les Systèmes Allaitants Multi-performants” (UMT SeSAM).

Appendix A. Supplementary data

Supplementary data to this article can be found online at https://doi.org/10.1016/j.ymeth.2020.06.014.

References

[1] N.C. Friggens, F. Blanc, D.P. Berry, L. Puillet, Review: Deciphering animal robustness A synthesis to facilitate its use in livestock breeding and management, Animal 11 (12) (2017) 2237–2251.

[2] J. Hervieu, P. Morand-Fehr, R. Delfa, Mise en place d'une echelle de notes caudales pour estimer l'etat corporel des chevres, Options Mediterraneennes Serie A, Seminaires Mediterranéens 27 (1995) 133–140.

[3] U.J. Schroder, R. Staufenbiel, Methods to determine body fat reserves in the dairy cow with special regard to ultrasonographic measurement of backfat thickness, J. Dairy Sci. 89 (1) (2006) 1–14.

[4] A.M. Scholz, L. Bunger, J. Kongsro, U. Baulain, A.D. Mitchell, Non-invasive methods for the determination of body and carcass composition in livestock: dual-energy X-ray absorptiometry, computed tomography, magnetic resonance imaging and ultrasound: invited review, Animal 9 (7) (2015) 1250–1264.

[5] J. Robelin, Cellularity of bovine adipose tissues developmental changes from 15 percent to 65 percent mature weight, J. Lipid Res. 22 (3) (1981) 452–457.

[6] F. Bocquier, P. Guillouet, F. Barillet, Y. Chilliard, Comparison of three methods for the in vivo estimation of body composition in dairy ewes, Ann. Zootech. 48 (4) (1999) 297–308.

[7] J. Robelin, Relation in vivo between the dilution space of deuteriated water and body water in growing cattle, Reprod. Nutr. Dev. 22 (1A) (1982) 65–73.

[8] P. Schmidely, J. Robelin, P. Bas, Comparaison de différentes méthodes d'interprétation de la prédiction de l'eau corporelle par la méthode de dilution de l'eau lourde : application chez le chevreau mâle, Reprod. Nutr. Dev. 29 (4) (1989) 487–494.

[9] C.T. Schaff, U. Pliquett, A. Tuchscherer, R. Pfuhl, S. Gors, C.C. Metges, H.M. Hammon, C. Kroger-Koch, Evaluation of electrical broad bandwidth impedance spectroscopy bioelectrical impedance spectroscopy as a tool for body composition measurement in cows in comparison with body measurements and the deuterium oxide dilution method, J. Anim. Sci. 95 (5) (2017) 2041–2051.

[10] L. Journaux, G. Renand, G. Longy, P. Baribault, Assessment of body composition in french beef cattle breeding schemes, using ultrasonic measurements with the VOS system 1999 INRA - Idele, Paris Rencontres Recherches Ruminants, 239–242.

[11] J.A. Mendizabal, R. Delfa, A. Arana, A. Purroy, A comparison of different pre- and post-slaughter measurements for estimating fat reserves in Spanish Blanca Celtiberica goats, Can. J. Anim. Sci. 90 (3) (2010) 437–444.

[12] P. Schmidely, P. Bas, P. Morand-Fehr, J. Hervieu, A. Rouzeau, Comparaison de 3 méthodes d'estimation de la composition corporelle des chèvres laitières sèches ou en lactation, Options Méditerraneennes Serie A, Séminaires Méditerranéens 27 (1995) 141–150.

[13] J. Hervieu, P. Colomer Rocher, A. Branca, R. Delfa, P. Morand-Fehr, Définition des notes d'état corporel des caprins., Réseau Agrimed-FAO de Recherches Coopératives sur les Productions Ovines et, Caprines Agrimed-FAO (1989) 5.

[14] A.G. West, S.J. Patrickson, J.R. Ehleringer, Water extraction times for plant and soil materials used in stable isotope analysis, Rapid Commun. Mass Spectrometry: RCM 20 (8) (2006) 1317–1321.

[15] J. Robelin, Estimation de la composition corporelle des animaux à partir des espaces de diffusion de l'eau marquée, Ann. Biol. Anim. Bioch. Biophys. 13 (2) (1973) 285–305.

[16] J.R. Speakman, G.H. Visser, S. Ward, E. Krol, The isotope dilution method for the evaluation of body composition, in: J.R. Speakman (Ed.), Body Composition Analysis of Animals: a Handbook of Non-Destructive Methods, Cambridge University Press Cambridge, UK, 2001, pp. 56–98.

[17] D.A. Schoeller, E. Ravussin, Y. Schutz, K.J. Acheson, P. Baertschi, E. Jequier, Energy expenditure by doubly labeled water: validation in humans and proposed calculation, Am. J. Physiol. 250 (5) (1986) R823–R830.

[18] C. Huau, A. Pommaret, D. Augerat, P. Marechal, L. Delattre, R. Rupp, L'imagerie 3D : une autre méthode d'évaluation de l'état corporel chez la chèvre Alpine, in: INRAE, Idele (Eds.) Rencontres Recherches Ruminants, Paris, 2020, in Press.

[19] Y. Le Cozler, C. Allain, A. Caillot, J.M. Delouard, L. Delattre, T. Luginbuhl, P. Faverdin, High-precision scanning system for complete 3D cow body shape imaging and analysis of morphological traits, Comput. Electron. Agric. 157 (2019) 447–453.

[20] Y. Le Cozler, C. Allain, C. Xavier, L. Depuille, A. Caillot, J.M. Delouard, L. Delattre, T. Luginbuhl, P. Faverdin, Volume and surface area of Holstein dairy cows calculated from complete 3D shapes acquired using a high-precision scanning system: interest for body weight estimation, Comput. Electron. Agric. 165 (2019).

[21] D. Legland, I. Arganda-Carreras, P. Andrey, MorphoLibJ: integrated library and plugins for mathematical morphology with ImageJ, Bioinformatics (Oxford, England) 32 (22) (2016) 3532–3534.

[22] C.A. Schneider, W.S. Rasband, K.W. Eliceiri, NIH Image to ImageJ: 25 years of image analysis, Nature Methods 9 (7) (2012) 671–675.

[23] A. Top, G. Hamarneh, R. Abugharbieh, Active learning for interactive 3D image segmentation, in: G. Fichtinger, A. Martel, T. Peters (Eds.), Medical Image Computing and Computer-Assisted Intervention - MICCAI, 2011, pp. 603–610.

[24] A. Top, G. Hamarneh, R. Abugharbieh, Spotlight: Automated Confidence-based User Guidance for Increasing Efficiency in Interactive 3D Image Segmentation Medical Image Computing and Computer-Assisted Intervention Workshop on Medical Computer Vision (MICCAI MCV), (2010), pp. 204–213.

[25] M. Monziols, J. Faixo, E. Zahlan, G. Daumas, Software for automatic treatment of large biomedical images databases, Proc. SCIA, Workshop on Farm Animal and Food Quality Imaging, Espoo, Finland, 2013, pp. 17–22.

[26] P. Bas, Y. Chilliard, P. Morand-Fehr, P. Schmidely, D. Sauvant, In vivo estimation of body lipid content of lactating goats based on the heavy water or the urea methods, Reprod., Nutr., Dev. (Suppl 2) (1990) 253s–254s.

[27] A.T. Ngwa, L.J. Dawson, R. Puchala, G. Detweiler, R.C. Merkel, I. Tovar-Luna, T. Sahlu, C.L. Ferrell, A.L. Goetsch, Urea space and body condition score to predict body composition of meat goats, Small Ruminant Res. 73 (1–3) (2007) 27–36.

[28] F.R. Dunshea, A.W. Bell, K.D. Chandler, T.E. Trigg, A two pool model of titrated water kinetics to predict body composition in unfasted lactating goats, Anim. Prod. 47 (1988) 435–445.

[29] D.L. Brown, S.J. Taylor, Deuterium oxide dilution kinetics to predict body composition in dairy goats, J. Dairy Sci. 69 (4) (1986) 1151–1155.

[30] S. Lerch, M.L. Lastel, C. Grandclaudon, C. Brechet, G. Rychen, C. Feidt, In vivo prediction of goat kids body composition from the deuterium oxide dilution space determined by isotope-ratio mass spectrometry, J. Anim. Sci. 93 (9) (2015) 4463–4472.

[31] J.R. Speakman, Body Composition Analysis of Animals: A Handbook of Non-Destructive Methods, Cambridge University Press Cambridge, UK, 2001.

[32] V.M. Thorup, D. Edwards, N.C. Friggens, On-farm estimation of energy balance in dairy cows using only frequent body weight measurements and body condition score, J. Dairy Sci. 95 (4) (2012) 1784–1793.

[33] V.M. Thorup, S. Højsgaard, M.R. Weisbjerg, N.C. Friggens, Energy balance of individual cows can be estimated in real-time on farm using frequent liveweight measures even in the absence of body condition score, Animal 7 (10) (2013) 1631–1639.

[34] J.A. Mendizabal, R. Delfa, A. Arana, A. Purroy, Body condition score and fat mobilization as management tools for goats on native pastures, Small Ruminant Res. 98 (1–3) (2011) 121–127.

[35] R.G. Vernon, Lipid metabolism in the adipose tissue of ruminant animals, Prog. Lipid Res. 19 (1–2) (1980) 23–106.

[36] A. Teixeira, M. Joy, R. Delfa, In vivo estimation of goat carcass composition and body fat partition by real-time ultrasonography, J. Anim. Sci. 86 (9) (2008) 2369–2376.

[37] J.A. Pires, Y. Chilliard, C. Delavaud, J. Rouel, D. Pomiès, F. Blanc, Physiological adaptations and ovarian cyclicity of Holstein and Montbéliarde cows under two low-input production systems, Animal 9 (12) (2015) 1986–1995.

[38] I. Donnem, M. Eknaes, A.T. Randby, Energy status, measured by computer tomography (CT)-scanning, and milk quality of dairy goats fed rations with various energy concentrations, Livest. Sci. 142 (1–3) (2011) 235–244.

[39] M. Eknaes, Y. Chilliard, K. Hove, R.A. Inglingstad, L. Bernard, H. Volden, Feeding of palm oil fatty acids or rapeseed oil throughout lactation: effects on energy status, body composition, and milk production in Norwegian dairy goats, J. Dairy Sci. 100 (9) (2017) 7588–7601.

[40] M.T. Sorensen, In vivo prediction of goat body composition by computer tomography, Anim. Prod. 54 (1992) 67–73.

[41] G. Aumont, F. Poisot, G. Saminadin, H. Borel, G. Alexandre, Body condition score and adipose cell size determination for in vivo assessment of body composition and post-mortem predictors of carcass components of Creole goats, Small Ruminant Res. 15 (1) (1994) 77–85.

[42] Y. Chilliard, M. Cisse, R. Lefaivre, B. Rémond, Body composition of dairy cows according to lactation stage, somatotropin treatment, and concentrate supplementation, J. Dairy Sci. 74 (9) (1991) 3103–3116.

[43] I. Chery, A. Zahariev, C. Simon, S. Blanc, Analytical aspects of measuring H-2/H-1 and O-18/O-16 ratios in urine from doubly labelled water studies by high-temperature conversion elemental analyser-isotope-ratio mass spectrometry, Rapid Commun. Mass Spectrom. 29 (7) (2015) 562–572.

[44] E.S. Berman, S.L. Fortson, S.P. Snaith, M. Gupta, D.S. Baer, I. Chery, S. Blanc, E.L. Melanson, P.J. Thomson, J.R. Speakman, Direct analysis of δ2H and δ18O in natural and enriched human urine using laser-based, off-axis integrated cavity output spectroscopy, Anal. Chem. 84 (22) (2012) 9768–9773.

[45] S.R. Silva, J. Afonso, A. Monteiro, R. Morais, A. Cabo, A.C. Batista, C.M. Guedes, A. Teixeira, Application of bioelectrical impedance analysis in prediction of light kid carcass and muscle chemical composition, Animal 12 (6) (2018) 1324–1330.